buildings

Review

Shear Strength of Ultra-High-Performance Concrete Beams without Stirrups—A Review Based on a Database

Yuan Huang [1,2,*] and Gaozhan Yao [1]

[1] College of Civil Engineering, Hunan University, Changsha 410082, China; gaozhanyao@hnu.edu.cn
[2] Hunan Provincial Key Laboratory on Damage Diagnosis for Engineering Structures, College of Civil Engineering, Hunan University, Changsha 410082, China
* Correspondence: huangy@hnu.edu.cn

Abstract: This paper presents a comprehensive study on ultra-high-performance concrete (UHPC) beams without stirrups, where the test data of 487 beams were collected, and an experimental database was established. Four distinct shear strength calculation models for UHPC beams were examined in the study. These models were created from national specification guides. The results indicate that while the code equation is useful for predicting UHPC beam shear capacity, it consistently underestimates actual values, with a mean experimental-to-calculated ratio above 1.5. The database was also used to study the impacts of the compressive strength of UHPC, the shear span-to-depth ratio, the fiber volume fraction, and the reinforcement ratio on the shear strength of UHPC beams. The findings showed that the shear span-to-depth ratio significantly affected the shear load-bearing capacity of UHPC beams. The increase in the compressive strength of UHPC, fiber volume fraction, and reinforcement ratio positively affected the shear strength of UHPC beams to varying degrees. Additionally, there were size effects for beams with a shear span-to-depth ratio of less than 1.5 and an effective depth of more than 300. In addition, coefficients accounting for fiber influence and the shear span-to-depth ratio were incorporated to develop an enhanced formula for UHPC beams. The empirical data from the database tests revealed that the average ratio of the beams' experimental shear capacity to the values predicted by the modified equation is 1.3, with a standard deviation of 0.74. These results suggest that the refined equation offers improved calculation precision and broader applicability. Eventually, a summary of the issues pertaining to the shear performance of UHPC beams and the key future research directions is provided to facilitate a clearer comprehension and awareness of emerging concepts for scholars within the discipline.

Keywords: UHPC; beam; shear strength; size effects; calculation models

Citation: Huang, Y.; Yao, G. Shear Strength of Ultra-High-Performance Concrete Beams without Stirrups—A Review Based on a Database. *Buildings* **2024**, *14*, 1212. https://doi.org/10.3390/buildings14051212

Academic Editor: George Morcous

Received: 14 March 2024
Revised: 20 April 2024
Accepted: 22 April 2024
Published: 24 April 2024

1. Introduction

Ultra-high-performance concrete (UHPC) has become a research hotspot in civil engineering, characterized by its comprehensive performance advantages [1–3]. UHPC is a brand-new cementitious material with a homogeneous ultrafine–dense system, excellent mechanical properties, and extensive design freedom [4–6]. UHPC's academic publications have increased exponentially in recent years, reflecting its unprecedented growth in the construction sector. To attain excellent mechanical qualities, UHPC is typically made using the maximum bulk density principle [7]. UHPC optimizes the internal pore structure and aggregate gradation, diminishes porosity, enhances compactness, and maintains a low water/cement ratio. In the fabrication of UHPC, the incorporation of steel fibers significantly improves tensile strength and mitigates self-desiccation shrinkage [8–13]. Moreover, UHPC possesses significantly elevated compressive strength, typically 3–16 times higher than standard concrete, with values commonly ranging from 150 to 810 MPa. [3,14,15]. Additionally, UHPC can withstand environmental erosion [16], demands less maintenance, and possess a longer service life than that of regular concrete, upon on its merit of low permeability [17,18].

In the realm of concrete infrastructure reinforcement and remediation, the advent of innovative materials has revolutionized the industry. Among these cutting-edge materials, UHPC, Steel-Reinforced Polymers (SRPs), and Fiber-Reinforced Polymers (FRPs) have garnered significant attention for their exceptional properties and versatile applications [19–22]. Zhang's experiments revealed that UHPC reinforcement in RC beams led to an 11.8–94.1% increase in shear cracking load and a 16–66.6% rise in ultimate shear capacity, compared to reference NC beams with equivalent shear span-to-depth ratios [23]. Moreover, by optimizing mix proportions and employing admixtures, UHPC can be formulated to be eco-friendly, cost-effective, and durable, meeting the criteria for challenging projects [24]. At the same time, advancements in numerical techniques are anticipated to enhance the precision of concrete design, efficiency in construction, and the overall performance of the material [25,26]. Hence, it is imperative to explore the behavior of UHPC and facilitate appropriate design methods for UHPC structures.

The shear resistance of concrete is a fundamental and complex issue related to its mechanical performance [27,28]. Nevertheless, the brittle shear behavior of concrete presents challenges in conducting corresponding experimental studies of shear behavior [29]. Even in conventional reinforced concrete structures, the shear behavior still poses many unresolved issues [30]. Despite this, the majority of the shear strength calculation approaches and models for UHPC members are empirical formulas that stem from experimental results and mathematical formulas, lacking explicit physical meaning [31]. Furthermore, the current research rarely focuses on the shear bearing capacity calculation of UHPC beams, and the shear theories of conventional RC are not suitable for UHPC beams [32,33]. UHPC is famous for its excellent mechanical properties and is utilized in many countries for major engineering structures [34–36]. A deep-seated exploration for clarifying the shear performance and shear damage mechanism of ultra-high-performance concrete members is demanded to better and more appropriately use them in practical engineering [37,38].

Scholars hailing from diverse countries have undertaken a variety of experimental investigations concerning the shear behavior of UHPC beams. The parameters investigated in these studies include the shear span-to-depth ratio, the volume admixture of steel fibers, the longitudinal reinforcement ratio, and the stirrup ratio [39,40]. The authors concentrated their efforts on gathering pertinent data from diverse regions pertaining to shear performance examinations of UHPC beams. The survey results indicated that 644 UHPC beams were tested, including 487 without stirrups and 157 stirrup-reinforced beams. In summation, the current body of research that focuses on the shear behavior of UHPC beams is primarily concerned with specimens without stirrups. Abundant research findings have demonstrated that the bridging effect of fibers within UHPC beams can significantly impede the propagation of shear cracks, thereby enhancing the shear resistance of the beams [10,41]. Moreover, to a certain degree, the fiber reinforcement can potentially eliminate the need for conventional web reinforcement entirely [42,43]. The findings from the present literature review indicate that while advancements have been achieved in the shear performance of UHPC beams, several issues and challenges persist. The variability in experimental data complicates the development of a unified shear calculation model. Furthermore, a comprehensive understanding of the impact of fibers on shear performance remains elusive, and the existing design codes and standards have not kept pace with the innovative applications of UHPC in structural engineering. These factors collectively restrict the broader implementation of UHPC in construction projects. This paper offers a comprehensive, data-driven analysis of the shear behavior in UHPC beams without stirrups, aiming to inform and assist professionals and researchers in the field of shear assessment.

2. Database Information

This paper presents a comprehensive experimental database of 487 UHPC beams. Some specimens characterized by incomplete information, compressive strengths of less than 100 MPa, and abnormal damage patterns are eradicated from the database. These specimens include 322 rectangular-section beams, 83 I-section beams, and 82 T-section beams, along with various parameters such as beam width (b), height (h), shear span-to-depth ratio (a/d), steel fiber volume fraction (V_f), longitudinal reinforcement ratio (ρ), and compressive strength of UHPC (f_c). In regard to testing parameters, the shear span-to depth ratio ranges from 0 to 8, the longitudinal reinforcement ranges from 0 to 9.47%, the fiber volume fraction from 0 to 4.7%, and the compressive strength of UHPC from 100 to 205 MPa. The detailed characteristics of the test specimens are delineated within Tables 1 and 2, while the distribution of their specific geometrical and material attributes is graphically represented in Figure 1. More details about the collected experiments can be found in the relevant references.

Table 1. UHPC beam database.

Num	Sec	f_c [MPa]	b [mm]	d [mm]	Type	V_f [%]	l_f/d_f	a/d	ρ [%]	Ref
1	Rec	125.3	200	306	SF	2	65	2	6.18	[37]
19	Rec	125–137	152	76–203	SF	2.1	72	0.8–2.8	2.2–7.8	[31]
9	Rec	127.1	150	219	SF	0–3	75	1.51–3.02	4.43–8.04	[44]
8	Rec	129.8–151.8	250	277	SF	2.65	65	1.5–3	5.6–7.1	[33]
1	Rec	118	150	260	SF	1	65	1.2	5.23	[45]
5	Rec	100–129	100	131	SF	0.5–2	40	2.5–3.5	4.1	[46]
1	Rec	151.4	150	542	SF	1	65	0.923	3.62	[47]
4	Rec	122.4	200	700–767	SF	2	59	1.17–1.96	1.08	[48]
1	Rec	166.9	150	220	SF	1.5	87	3	0.78	[49]
6	Rec	100–122	180	150–490	SF	0–3	45	2	2.1	[50]
45	Rec	180	50	50	SF	0.5–1.5	95	0–0.7	0	[51]
3	Rec	100–200	200	300	SF	0–2	40	2	4.09	[52]
9	Rec	134.5	120	150–270	SF	0.4	80	1–2	3.9–4	[53]
7	Rec	116.85	110	250	SF	2	52	1.25–2	2.44	[54]
1	Rec	125	200	250	SF	3	65	2	5.5	[26]
1	Rec	118	150	175	SF	1	65	1.2	5.23	[55]
9	Rec	107–131	150	175–200	SF	1–3	75	1.51–3.02	4.43–8.04	[56]
24	Rec	100–143	165	260	S + P	0–2.25	65/210	1.5–3.3	7.5	[57]
15	Rec	126–140	100	124	H + DH	0–1.5	37/80	4.03	5.07	[58]
13	Rec	100–122	100	167	SF	0.4	80	1–3	1.35–6.1	[59]
17	Rec	100–159	100	112	SF	0.5–2	65	2.5–4.5	3.4–5.9	[60]
6	Rec	126–159	200	224.5	SF	0–2	80	1.2–3.1	3.27	[61]
5	Rec	103–122	120	170	SF	0–2	95	2.5–3	4	[62]
3	Rec	132–143	250	270	SF	2.65	65	1.5–3.5	7.1	[63]
8	Rec	117.6–119.3	170	210	SF	2–3	65	1.4–3.2	8.15	[64]
16	Rec	147–166	350	130–160	SF	2	65	1–2.5	4.14	[65]
6	Rec	127	150	200	SF	2	50	1.51–2.26	4.4–8.0	[66]
8	Rec	127–151	150	200	SF	2	65	1–3	4.4–8.2	[67]
3	Rec	134.6	150	200	SF	2	76	1–3	8.18	[68]
3	Rec	124.9	150	280	SF	3	39	1.61–2.7	2.2–3.1	[69]
3	Rec	100–106	110	130	SF	1	80	3.27	1.58–2.37	[70]
6	Rec	118–126	100	130	S + P	0–0.5	13/65	2	1.2–1.7	[71]
14	Rec	136–151	100	130	SF	0.34–1.25	64	2.3	2.8–4	[72]
16	Rec	126–152	100	127	H + DH	0–1.5	37/80	3.9	2.4	[73]
18	Rec	165.7–180	150	75–125	SF	3	65	1–2	0.5–2.0	[74]
8	Rec	136–145	250	300	SF	2.65	65	2–3	5.6–7.1	[75]
7	T	113–121	40	114	SF	2	30/65	2.5–3.17	4.96	[76]
11	T	103–156	140	240	S + B	0–1.5	60	2–3	2.87	[77]
6	T	108–138	80	297	SF	0–3	65	1–3	2.97	[42]
7	T	152–167	60	302	SF	1–2	65	1–3.5	8.66	[78]
6	T	113–136	40	114	SF	2	30/65	2.5–3.75	4.96	[79]
1	T	128	70	440	SF	1	65	2.75	3.4	[80]
1	T	149	60	430	SF	1.5	59	2	9.47	[81]
3	T	116–120.5	40	114	SF	2	30/65	3.17	4.96	[82]
7	T	152–167	60	302	SF	1–2	65	1–3.5	8.66	[83]
2	T	132–137	50	265	SF	1.8	75	2–3	1.9	[84]
3	T	125	40–80	130–265	SF	0.75	65	2.5	5.9	[85]
8	I	144–152	50	315–397	SF	1–3	65	4–8	3.5–5	[86]
9	I	160–188	60	315	SF	1–2	75	3.55	5.1	[87]
6	I	121–143	50	230	SF	0–2	55	3.1	0.8–2.2	[88]
12	I	136–155	50	223	SF	1.5–2.55	63	1.25	1.15	[89]
4	I	120–141	55	195	SF	2	44/73	2.5	5.9	[90]
7	I	157–205	65	305	SF	0–4.7	65	2.5	3.84	[91]
3	I	141–148	50	350	SF	0–1.6	65	2.85	5.5	[92]
—	—	140	121	233	—	1.54	66	2.24	4.05	Average
—	—	205	350	800	—	4.7	210	8	9.47	Maximum
—	—	100	40	50	—	0	0	0	0	Minimum

Note: Rec = rectangular section; T = T-shaped section; I = I-shaped section. Type of fibers = SF for steel fibers, S + P for steel fibers and PVA fibers, H + DH for end-hooked steel fibers and double end-hooked steel fibers, and S + B for steel fibers and basalt fibers.

Table 2. Prestressed UHPC beam database.

Num	Sec	f_c [MPa]	b [mm]	d [mm]	Type	V_f [%]	l_f/d_f	a/d	ρ [%]	σ_p [MPa]	Ref
8	T	163–179	50	250	SF	1–2	65	1–1.5	1–3	6.7–12.3	[93]
3	T	145–175	50	360	SF	2.5	65	1.44–3.67	0.52–2.54	16.6–17.5	[94]
5	T	151–183	60	316	SF	0.9–2.5	117	3.8–4.4	0.9–2.5	37.8–43.5	[95]
7	T	163–179	50	250	SF	1–2	65	1–1.5	1–3	6.7–12.4	[96]
5	T	150–161	40	182	SF	2	65	2.8–4.5	4.66	3.8–35.3	[97]
8	I	122–140	50	620	SF	1–1.5	75/125	1.75–4.5	1.07	30.96	[98]
7	I	141–169	50	600	SF	1.25–2.5	65	3.23	1.83	32	[99]
7	I	111–125	70	350	SF	0.75	65	1.29–2.57	2.01	6.5–14.2	[100]
12	I	167–193	50	640	SF	1–2	65	2.5–3.4	1.12	44.5–49.5	[101]
—	—	159	52	475	—	1.55	72	2.59	1.83	24.2	Average
—	—	193	70	700	—	4.7	125	4.5	4.66	49.5	Maximum
—	—	111	40	200	—	0	60	1	0.52	3.8	Minimum

Note: σ_p for prestressing values of test beams.

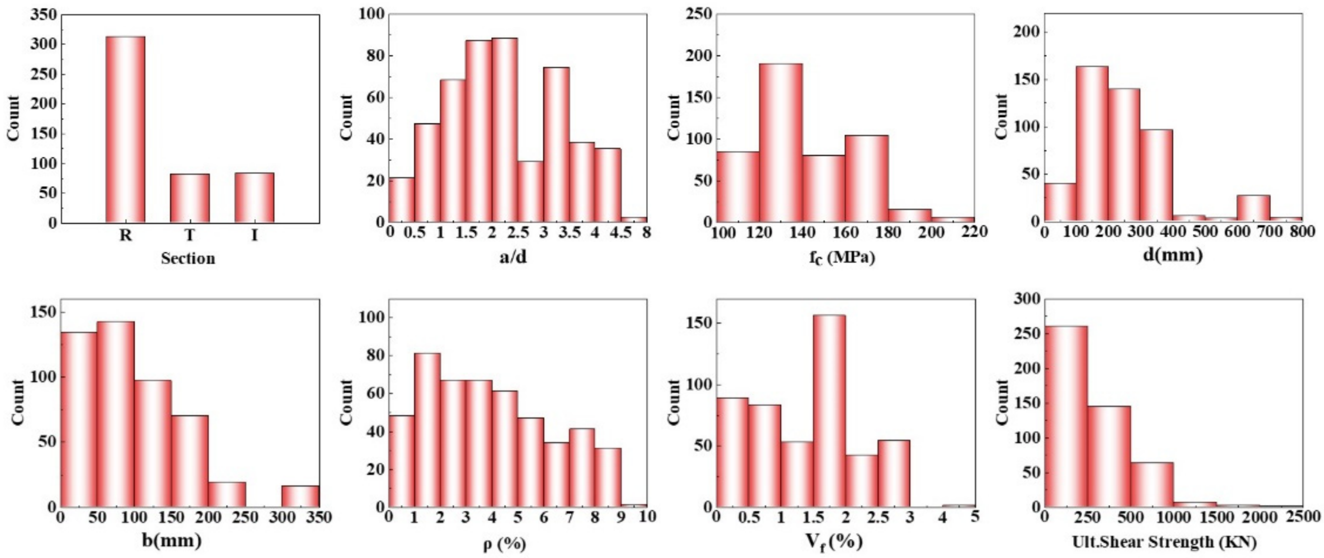

Figure 1. Distribution of the material and geometric properties of the UHPC beams in the database.

3. Factors Affecting the Shear Strength of UHPC Beams

Existing studies demonstrate that the shear performance of UHPC beams is dominated by several factors, primarily encompassing the shear span-to-depth ratio, fiber volume fraction, longitudinal reinforcement ratio, and stirrup rate [102–104]. Consequently, the above parameters were focused on and collected while collecting data from the database. The relationships between these influencing factors and the shear behavior were meticulously examined, and the corresponding correlation curves have been graphically represented (refer to Figure 2).

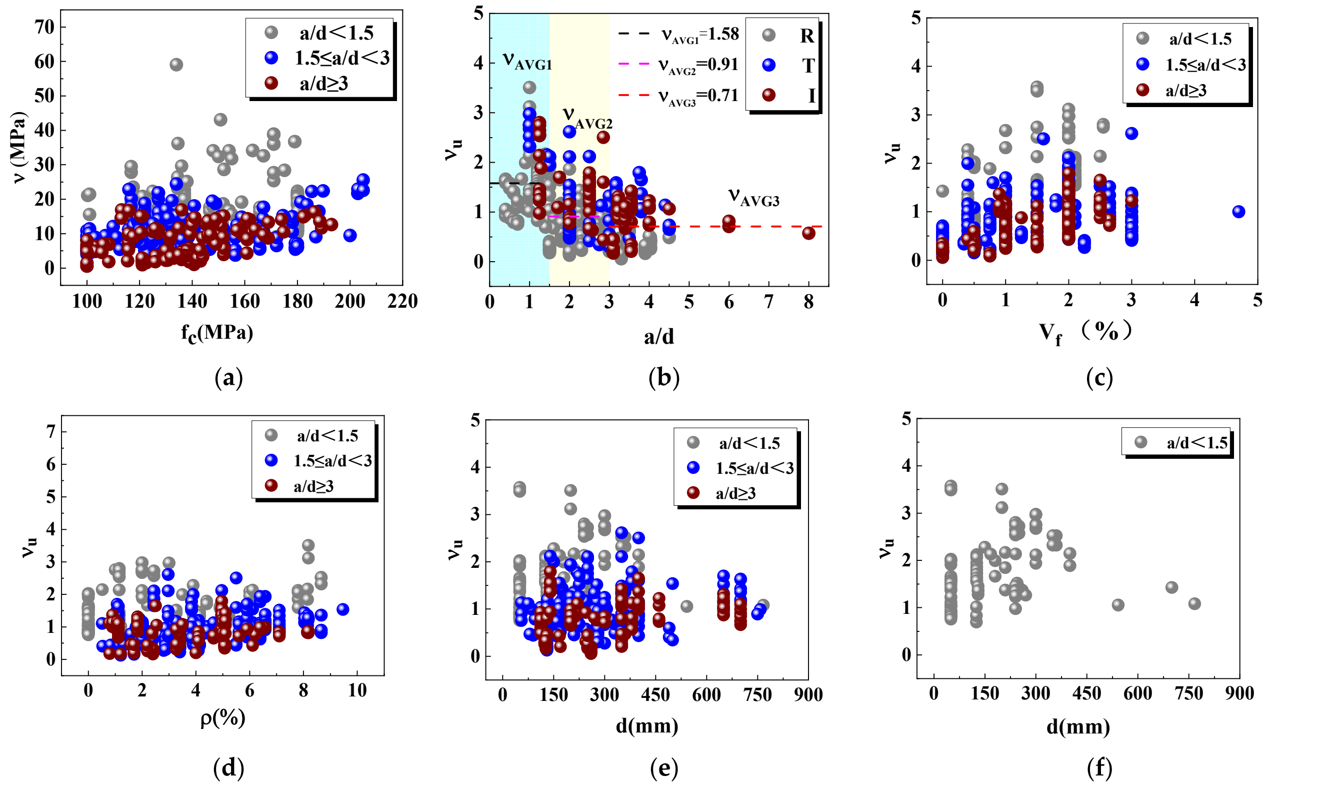

Figure 2. Scatter plots of the nominal or normalized shear strength of the beam versus (**a**) compressive strength of UHPC, (**b**) shear span-to-depth ratio, (**c**) fiber volume fraction, (**d**) longitudinal reinforcement ratio, (**e**) effective depth, and (**f**) effective depth (a/d < 1.5).

3.1. Compressive Strength of UHPC

In respect of compressive strength, the shear capacity is determined by taking the nominal shear strength (ν) of the beam cross-section. Simultaneously, to mitigate the impact of compressive strength on the shear capacity of UHPC beams during the analysis of other parameters, the standardized shear strength (ν_u) is utilized. Equations (1) and (2) represent ν and ν_u, respectively [105]. Figure 2a illustrates the correlation between the nominal shear strength of UHPC beams and the compressive strength of UHPC cubes. The nominal shear strength is observed to increase with the enhancement of UHPC's compressive strength, a phenomenon attributed to the concurrent improvement in tensile strength, which inhibits crack propagation within the beam. For the beams without stirrups, when the ratio of shear span to depth (a/d) is greater than or equal to 3, the nominal shear strength is primarily distributed in the range of 0–10 MPa. When 1.5 < a/d < 3, the majority of nominal shear strengths fall between 5 and 15 MPa. For cases where a/d is less than or equal to 1.5, the nominal shear strength is generally greater than 15 MPa. This indicates that beams with smaller shear span ratios contribute significantly to shear resistance, resulting in higher shear carrying capacities.

$$\nu = V_u/bd \tag{1}$$

$$\nu_u = V_u/bd\sqrt{f_c} \tag{2}$$

3.2. Shear Span-to-Depth Ratio

Regarding the shear capacity of reinforced concrete beams, the shear span-to-depth ratio reflects the relative percentage of bending moment to shear force in the area to some extent. The shear span-to-depth ratio, which typically plays a decisive role in the damage pattern, has a considerable effect on the shear bearing capacity [106,107]. Figure 2b illustrates the relationship between standardized shear strength and the shear span-to-depth ratio of UHPC test beams. It can be observed that with the increase in the shear span-to-depth ratio (a/d), the standardized shear strength declines. When a/d exceeds 3, this trend tends to stabilize, consistent with the pattern of shear strength reduction with shear span to depth observed in conventional concrete beams [108]. Through the processing of data from all test specimens, the average shear carrying capacity of the test beams is approximately $1.1\sqrt{f_c}bd$, which is significantly higher than the shear carrying capacity of conventional concrete beams, which is $0.17\sqrt{f_c}bd$ [105]. In comparison with ordinary concrete, UHPC beams exhibit outstanding shear carrying capacity.

3.3. Steel Fibers

UHPC is commonly utilized in conjunction with steel fibers, which extensively enhance the performance of UHPC much better. Additionally, fiber incorporation has a non-negligible contribution to the shear properties of UHPC beams [109,110]. The current study concluded that the volume dosage of steel fibers is generally in the range of 0% to 3% [41]. The increase in fiber doping conspicuously improves the flexural stiffness and deformation capacity of beams, and the variation in steel fiber doping also induces the changes in the damage morphology of the tested beams [48,111]. As shown in Figure 2c, which illustrates the relationship between standardized shear strength and steel fiber volume fraction, the standardized shear strength of UHPC beams indeed increases with the higher steel fiber volume fraction, following a stabilizing level or slight drop trend. Moreover, the larger the shear span-to-depth ratio, the more pronounced the enhancement effect of fibers on the shear carrying capacity. This phenomenon can be explained by the fact that the failure mode of beams with small shear span ratios tends to be inclined toward compression failure, where the majority of shear forces depend on the compressive strength of the concrete in the shear-compression zone, and the influence of fibers on the compressive strength of concrete is limited.

3.4. Reinforcement Ratio

The research indicates that the longitudinal reinforcement ratio influences the shear capacity of UHPC beams, with higher ratios marginally improving shear strength, yet the effect plateaus at a certain point [32,33,47,55]. Concurrently, an elevated reinforcement ratio is correlated with reduced cracking loads, while additional longitudinal reinforcement at the beam's base impedes vertical crack propagation, leading to the formation of diagonal cracks in bending and shear regions [56,112]. Figure 2d depicts the relationship between standardized shear strength and the longitudinal reinforcement ratio; the conclusion shows that the standardized shear strength exhibits an increasing trend with the increase in the longitudinal reinforcement ratio. The two variables demonstrated a closely linear relationship, indicating a noticeable anchorage effect of longitudinal reinforcement in UHPC beams without stirrups. Even when the longitudinal reinforcement ratio is relatively large, the degree of increasing ν_u is not infinite, suggesting that the anchorage effect of longitudinal reinforcement in UHPC beams is restricted to some extent.

3.5. Effective Depth

Research data from different scholars indicate that the effective height of beams influences their shear and flexural performance, with this impact being moderated by the shear span-to-depth ratio [50,85,113]. Moreover, an increased steel fiber volume fraction reduces the size effect in UHPC members, enhancing ductility, especially in beams with heights under 300 mm [114–116]. As shown in Figure 2e,f, regarding the specimens carried with shear span ratios greater than 1.5, no apparent relationship between the standardized shear strength and the effective depth is explored. Conversely, some specimens with shear span ratios less than 1.5 exhibit a significant size effect, but only when the effective depth of the beam is greater than 300. The analysis concludes that the standardized shear strength would decrease with the increase in effective depth. Regretfully, in the light of the restricted data resources and the various influencing factors among specimens, further research and evaluation would be required to fully illustrate the impact of size effects in future work.

4. Assessment of Code Shear Equations

4.1. Code Equations

The factors affecting the shear capacity of reinforced concrete beams are varied and the elements interact with each other. Extensive pilot studies have been conducted by researchers from various countries to propose appropriate design guidelines. Currently, the main UHPC design guidelines cover the French UHPC guidelines (AFGC-2016 [117]), the Japanese UHPC structural design and construction guidelines (JSCE2006 [118]), the Swiss UHPC standard (SIA2016 [119]), and the Korean UHPC design guidelines (KCI-2012 [120]).

4.1.1. France UHPC Design Guide AFGC-2016

In the context of the classical truss model, AFGC-2016 [117] employs a calculation model for shear bearing capacity. The AFGC-2016 model takes into account the contribution of stirrups using the variable angle truss model. Additionally, the shear contribution of the steel fibers incorporated in the UHPC is also calculated in the model. The shear bearing capacity calculation formulas are presented as Equations (3)–(6).

$$V_u = V_c + V_s + V_f \tag{3}$$

$$V_c = \frac{0.21}{\gamma_{cf}\gamma_E} k f_c^{\frac{1}{2}} b_w d \tag{4}$$

$$V_s = \frac{A_{sv}}{s} z f_{yv} \cot\theta \tag{5}$$

$$V_f = A_b \sigma_f \cot\theta \tag{6}$$

where $\gamma_{cf}\gamma_E$ is a safety factor, taking the value of 1.5, and k is the prestressing influence factor. f_c is the compressive strength characteristic value. b_w is the minimum width of the cross-section of the stretch zone. d is the maximum distance between the compression fiber and the longitudinal reinforcement. A_{sv} is the stirrup area. z is the distance between the points of merging of the longitudinal bars at the upper and lower edges of the member's section. θ is the angle between the concrete diagonal compression web and the beam axis in the joist model. A_b is the cross-sectional area of the beam. σ_f is the residual tensile strength of UHPC after cracking for ease of calculation and can be taken as 7 MPa [121].

4.1.2. Japan UHPC Design Guide JSCE-2006

JSCE-2006 [118] employs a shear bearing capacity calculation method that comprises three components: the contribution of the UHPC matrix, stirrup, and steel fiber. The specific calculation equations for each component are presented in Equations (7)–(11).

$$V_u = V_c + V_s + V_f + V_p \tag{7}$$

$$V_c = 0.18\sqrt{f_c} b_w d / \gamma_b \tag{8}$$

$$V_s = [\frac{A_{sv} f_{yv} (\sin\alpha + \cos\alpha)}{s}] z / \gamma_b \tag{9}$$

$$V_f = (f_t / \tan\theta) b_w z / \gamma_b \tag{10}$$

$$V_p = p_{ed} \sin\alpha_p / \gamma_b \tag{11}$$

where b_w represents the section width, d is the effective depth of the member, γ_b is the safety factor (taken as 1.3), α is the angle between the shear reinforcement and the axis, z is the distance from the compressive stress concentration point to the center of mass of the tensile reinforcement (usually taken as $d/1.15$), θ refers to the angle between the oblique cracks on the surface of the member and the axis of the member (taken as 45°), and p_{ed} indicates the effective tension of the longitudinal prestressing reinforcement.

4.1.3. Swiss UHPC Standard SIA2016

SIA2016 specifies that for structural elements constructed using UHPFRC [119], the shear design value of the original element should be determined by combining the shear strength of the UHPFRC with the shear resistance of the shear reinforcement. The ultimate shear resistance design value is calculated using Equations (12)–(14).

$$V_u = V_c + V_s \tag{12}$$

$$V_c = \frac{0.5bz(f_{Uted} + f_{Utud})}{\tan\theta} \tag{13}$$

$$V_s = \frac{A_s}{s} z f_y [\cot\theta + \cot\alpha] \sin\alpha \tag{14}$$

where f_{Uted} and f_{Utud} are the design values of the elastic tensile strength and ultimate tensile strength of UHPC, respectively, and α is the angle between the tensioned web and beam axes in the joist model.

4.1.4. Korea UHPC Design Guide KCI2012

KCI2012 [120] presents shear strength equations for beam members that are based on the same principles recommended by JSCE. Thus, the design shear strength is primarily obtained using Equations (7), (15)–(18).

$$V_c = \phi_b \left(0.18\sqrt{f_c} bd\right) = 0.139\sqrt{f_c} bd \tag{15}$$

$$V_s = \phi_b \frac{f_{svy} A_{sv} (\sin\theta_1 + \cos\theta_1)}{s} z \tag{16}$$

$$V_f = \frac{0.67bh f_{fav}}{\tan\theta} \tag{17}$$

$$V_p = \phi_b p_e \sin\alpha \tag{18}$$

where ϕ_b is the component discount factor, usually taken as 0.77; d represents the effective depth of the specimen; z is the distance from the compressive stress concentration point to the center of mass of the tensile reinforcement, usually taken as $d/1.15$; θ is the angle between the main crack of the beam and the horizontal axis, which is 45° for the convenience of calculation; θ_1 is the angle between the shear reinforcement and the horizontal axis in the beam; f_{fav} is the average design tensile strength; p_e represents the effective tension of the longitudinal reinforcement; and α is the angle between the longitudinal reinforcement and the axis of the member.

The current codes nearly employ section-based shear design formulas, composed of linear combinations of contributions from concrete shear, stirrup shear, and fiber shear. All codes cover parameters such as web width, effective depth, and the shear reinforcement ratio. Nevertheless, there are variations in the consideration of other parameters, as shown in Table 3. From the previous analysis of the main influencing factors in the UHPC beam database, it is evident that the shear span-to-depth ratio significantly influences shear carrying capacity. The current code calculation formulas not touch upon the function of the shear span-to-depth ratio. Except for SIA, which considers the tensile strength of UHPC, the strength considerations in the specifications of other countries all adopt a power function of compressive strength. None of the design methods attach importance to the longitudinal reinforcement ratio and size effects. All mentioned calculation methods consider the influence of fibers, but the consideration forms vary. The general idea is to separately calculate the shear contribution of fibers based on the tensile strength of UHPC.

Table 3. Comparison of main influencing factors in different code design formulas.

Code	a/d	Compressive Strength	Reinforcement Ratio	Size Effect	Steel Fibers
AFGC [117]	/	$\sqrt{f_c}$	/	/	σ_f
JSCE [118]	/	$\sqrt{f_c}$	/	/	f_t
SIA [119]	/	$f_{Uted} + f_{Utud}$	/	/	$f_{Uted} + f_{Utud}$
KCI [120]	/	$\sqrt{f_c}$	/	/	f_{fav}

4.2. Model Comparison

Theoretical calculations of the shear bearing capacities of the UHPC beams in the test database were performed using the theoretical calculation models mentioned earlier. The experimental and calculated values' relationships were plotted under different theoretical models. Figure 3 shows the results, where the dashed line represents a ratio of one between the theoretical and test values. The points in the graph represent experimental data, and the closer the data points are to the dashed line, the more accurate the formula calculations. The statistical indicators of the predicted results from different code formulas are shown in Table 4.

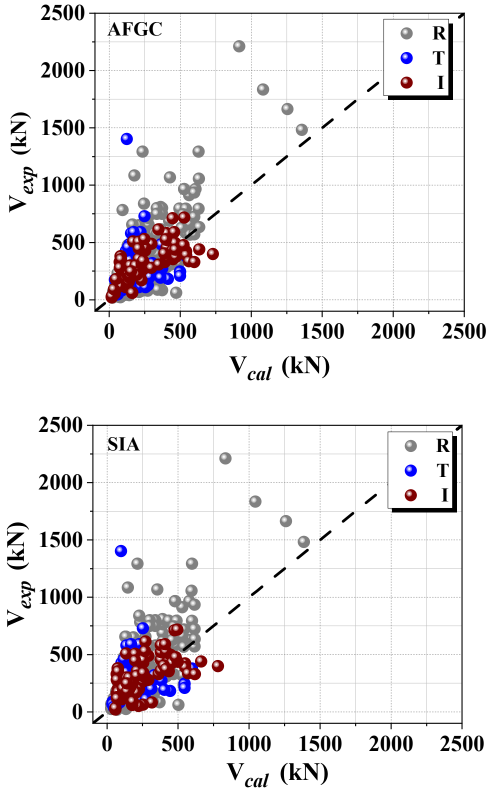

Figure 3. Results of different code models.

Table 4. Statistics indicators for shear strength prediction results.

Code	ξ_a	ξ_{sd}	R	$\xi_{\max}$	$\xi_{\min}$
AFGC [117]	1.59	1.18	0.74	11.95	0.13
JSCE [118]	1.71	1.24	0.73	12.59	0.14
SIA [119]	1.55	1.19	0.77	14.23	0.12
KCI [120]	1.99	1.41	0.71	14.49	0.17

Note: $\xi = V_{\text{exp}}/V_{cal}$, ξ_a: the average of ξ; ξ_{sd}: the standard deviation of ξ; R: the coefficient of variation of ξ; $\xi_{\max}$: the maximum value of ξ; $\xi_{\min}$: the minimum value of ξ.

Overall, from Figure 3 and Table 4, it can be observed that the ξ values for all four calculation methods are greater than 1, indicating varying degrees of conservative estimates for the shear carrying capacity of UHPC beams without stirrups. Through a comprehensive comparison of these four calculation methods, the French code with $\xi_a = 1.59$ and $\xi_{sd} = 1.18$ yields the smallest prediction errors and dispersion. The calculation methods in the Japanese and South Korean codes are similar to the French code, with differences only in the safety factor introduced in the concrete matrix term. The Swiss code combines the matrix term and the fiber term, forecasting the shear capacity through the tensile strength of UHPC.

5. Improved Shear Equations for UHPC Beams

Based on the aforementioned discussions, it is evident that existing shear equations for UHPC beams without stirrups are either overly conservative or unsafe in comparison with the tested results. Therefore, this study further continues to propose an improved model to forecast the shear strength of UHPC beams.

5.1. Parameter Design

To begin with, based on the data available in the experimental database, a correlation matrix between various influencing parameters and shear carrying capacity is generated (seen in Figure 4). The heat map of the correlation matrix for the influencing factors shows that the correlation coefficients between the different factors are small (except for the longitudinal reinforcement ratio); i.e., the effect on the shear capacity assessment is relatively small [26]. In addition, the correlation coefficients between the width and effective depth of the beam section, as well as the shear span-to-depth ratio, the fiber volume fraction, and the shear capacity, are relatively large; i.e., they have a significant effect on the shear capacity of the beams, whereas the effect of the compressive strength is relatively small. From the aforementioned analysis in Section 3, the shear carrying capacity of UHPC beams without stirrups increases with the enhancement of the compressive strength, longitudinal reinforcement ratio, and fiber volume fraction. However, it decreases with the rise of the shear span-to-depth ratio. Importantly, UHPC beams exhibit a significant size effect, particularly in the context of smaller shear span-to-depth ratios. In the comparison of the main influencing factors in the prescriptive formulas in Table 3, it is evident that none of the four code assessment approaches sufficiently balance the influence of factors such as the shear span-to-depth ratio and fiber volume fraction on the shear carrying capacity.

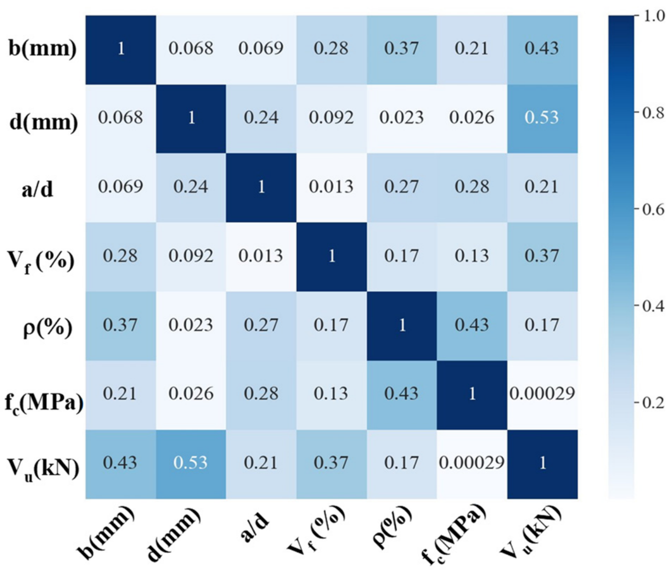

Figure 4. Heat map of correlation between shear capacity and influencing parameters.

5.2. Shear Mechanism in Inclined Sections

Shear failure is characterized by the occurrence and development of inclined cracks, and sometimes, once inclined cracks appear, the component may fail immediately. Compared to ordinary concrete beams, the bonding between steel fibers and the UHPC matrix in UHPC beams can effectively inhibit the development and propagation of inclined cracks [122]. Additionally, the bridging effect of fibers across cracks can provide a new pathway for shear force transmit [41,123]. A force diagram for the inclined section of a UHPC beam without stirrups is illustrated in Figure 5. The resistance on the inclined section primarily consists of the following components: shear carrying capacity provided by the shear-compression zone of UHPC (V_c); shear carrying capacity provided by the anchorage effect of longitudinal steel reinforcement (V_d); aggregate interlock force generated when concrete on both sides of the inclined crack undergoes sliding (V_a); and shear carrying capacity provided by the bridging action of fibers at the inclined crack (V_f). The shear carrying capacity of a UHPC beam without stirrups is given by Equation (19).

$$V_u = V_c + V_d + V_a + V_f \tag{19}$$

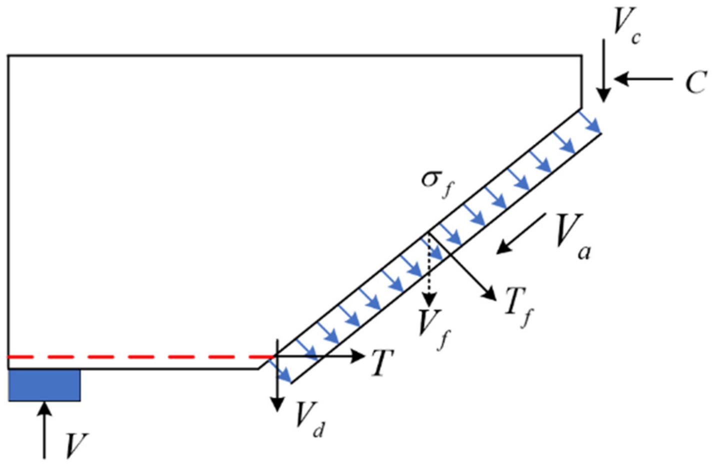

Figure 5. Shear force analysis diagram of inclined section of UHPC beam without stirrups.

5.3. Modified Equation Considering the Contribution of the Steel Fibers

Regarding the shear carrying capacity of UHPC beams, the shear resistance that stems from steel fibers primarily comes from the fibers crossing the main crack. During shear failure, majority of fibers within main cracks are pulled out, and the shear contribution of the fibers along the main crack is equivalent to the tension force when the fibers are pulled out. In order to accurately reflect the influence of parameters including fiber orientation, embedment depth, and matrix bonding strength at the main inclined crack of UHPC beams under shear loading, a mesoscale fiber–matrix discrete model (MFDM) [79,124] is proposed. In essence, parameters such as the effective width of fiber distribution, the pull-out force of a single fiber, and the number of fibers within the effective fiber distribution area should be considered when the shear contribution of fibers at the main inclined crack are calculated. Therefore, through simplification and derivation, the shear contribution of fibers (denoted as V_f) can be obtained as shown in Equation (20).

$$V_f = 0.45\tau_f \rho_f \frac{l_f}{d_f} bd \cot\theta \tag{20}$$

where τ_f represents the bonding strength at the fiber–matrix interface; ρ_f represents the volume fraction of fibers; l_f/d_f represents the aspect ratio of fibers.

Based on the above analysis, the fundamental form of the fiber contribution shear carrying capacity formula, incorporating parameters such as fiber content characteristics and fiber–matrix interface bonding strength, can be expressed as Equation (21). Let α_f be the shear capacity coefficient for inclined-section steel fibers, which is a function correlated with the fiber content characteristic value, λ_f.

$$V_f = \beta_v k \lambda_f bd\sqrt{f_c} \quad (21)$$

where the fiber–matrix interface bonding strength can be taken according to Singh's [125] recommendation, $\tau_f = k\sqrt{f_c}$; β_v represents the comprehensive coefficient that accounts for factors such as the random distribution of fibers and their effectiveness; λ_f represents the characteristic value of fiber content, $\lambda_f = \rho_f l_f / d_f$; $\alpha_f = \beta_v k \lambda_f$.

As analyzed in the fourth section, among several codes, the French code exhibits good accuracy, consistency, and safety margins in predicting shear capacity. Therefore, the bearing capacity equations for the fiber term can be fitted utilizing the shear data for UHPC beams without stirrups in Section 4 in accordance with the formula $\alpha_f = V_f / bd\sqrt{f_c}$, where the fiber term can be determined using the difference between the tested value of the shear capacity and the calculated value of the shear capacity of the substrate in the French code. During the fitting procedure, with reference to the experience of ordinary concrete specification, the value of α_f is considered, with a guarantee rate of about 85%, and the expression of α_f obtained from the fitting is $\alpha_f = 0.4\lambda_f$; a comparison of the predicted results with the test values of the shear capacity of the fiber term is shown in Figure 6. The final formula for the modified fiber's contribution to the shear bearing capacity is obtained as Equation (22).

$$V_f = 0.4\lambda_f bd\sqrt{f_c} \quad (22)$$

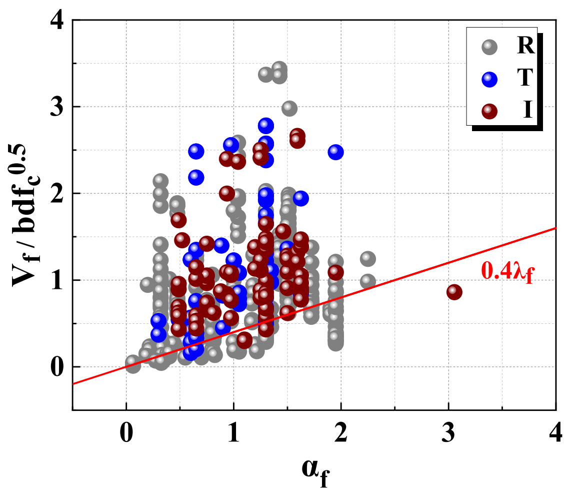

Figure 6. Comparison of fiber coefficients of inclined sections.

5.4. Modified Equation Considering the Shear Span-to-Depth Ratio

To consider the effect of the shear span-to-depth ratio on the shear bearing capacity of UHPC beams without stirrups, under the guidance on the effect of the shear span-to-depth ratio in Chinese specification DBJ 43/T 325-2017 [126], it is assumed that the formula for calculating the shear bearing capacity of UHPC beams without stirrups, which takes into account the effect of the shear span-to-depth ratio, is Equation (23):

$$V_u = \alpha_{cv}(0.21\sqrt{f_c}bd/\gamma_{cf}\gamma_E + 0.4\lambda_f\sqrt{f_c}bd) \quad (23)$$

where α_{cv} is the shear capacity coefficient of the diagonal cross-section of the UHPC beam without stirrups considering the effect of the shear span-to-depth ratio, which is a function related to the shear span-to-depth ratio.

The shear load capacity equations considering the effect of the shear span-to-depth ratio are also fitted using the shear test data for UHPC beams without stirrups in Section 4. The influence coefficient of the diagonal section considering the shear span-to-depth ratio, α_{cv}, can be determined as the ratio of the tested and calculated values of the shear capacity of the UHPC beam, i.e.,$\alpha_{cv} = V_e/V_c$, where α_{cv} is the segmental function related to the shear span-to-depth ratio. A comparison of the predicted results with the test values of the shear capacity of the UHPC term is shown in Figure 7, and the final formula for the shear capacity of the corrected UHPC beam without stirrups is obtained as Equation (24).

$$V_u = \begin{cases} 1.8(0.21\sqrt{f_c}bd/\gamma_{cf}\gamma_E + 0.4\lambda_f\sqrt{f_c}bd) & a/d \le 1.5 \\ \frac{5.4}{1.5+\lambda}(0.21\sqrt{f_c}bd/\gamma_{cf}\gamma_E + 0.4\lambda_f\sqrt{f_c}bd) & 1.5 < a/d < 3 \\ 1.2(0.21\sqrt{f_c}bd/\gamma_{cf}\gamma_E + 0.4\lambda_f\sqrt{f_c}bd) & a/d \ge 3 \end{cases} \quad (24)$$

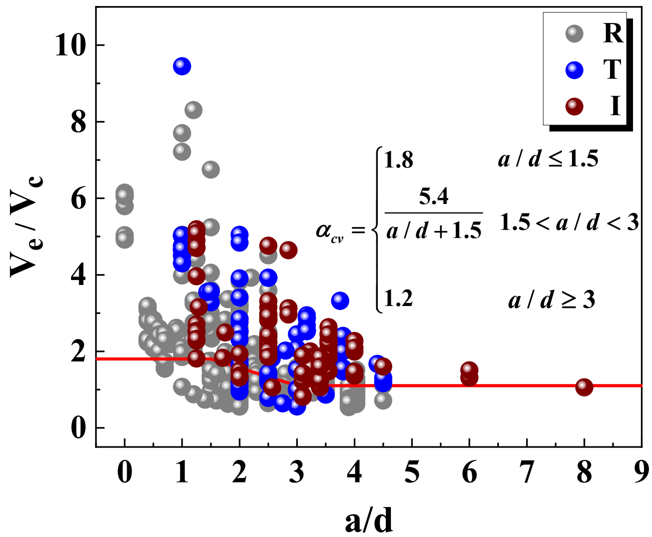

Figure 7. Comparison of shear span-to-depth coefficients for inclined sections.

5.5. Performance of the Proposed Shear Equation

The test data in the database were evaluated through the fitted equation and the results are shown in Figure 8. The relevant coefficients are as follows: the mean value of the ratio of the test values to the calculated values is 1.3, the standard deviation is 0.74, the coefficient of variation is 0.57, the maximum value is 5.25, and the minimum value is 0.26. In contrast to the four canonical calculation approaches, the data points calculated by the fitted formula are regularly distributed along the 45° line, and the degree of dispersion is further reduced. In summary, the proposed equation can assess more consequences related to the shear capacity of UHPC beams without stirrups than existing equations.

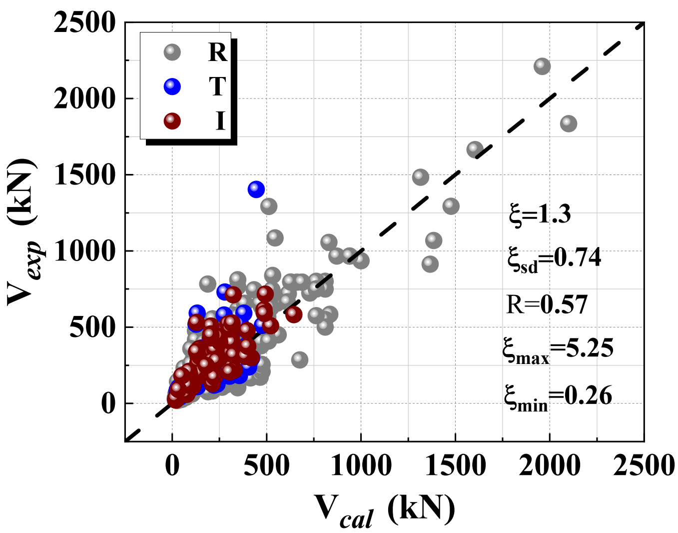

Figure 8. Results of the proposed shear equation.

6. Conclusions

In this study, a database of 487 UHPC beams without stirrups is established based on the collected shear performance test data and the impact of diverse parameters on the shear performance of UHPC beams is discussed. The shear capacity of the tested beams was compared and analyzed with the theoretically calculated values using the theoretical calculation models from the UHPC design guidelines of four countries. The main findings are as follows:

The shear capacity of UHPC beams diminishes with increasing shear span-to-depth ratio, while the fiber volume fraction and longitudinal reinforcement ratios positively correlate with shear strength. The shear span ratio is the primary influencing factor, followed by fiber dosage. A significant size effect is noted for UHPC beams with low shear span ratios and heights over 300 mm, differing from ordinary concrete and necessitating further study.

All four UHPC codes follow the sub-stacking concept, which accounts for the shear contributions from both the UHPC matrix and the fibers, to estimate the shear capacity. The analysis of the database assessment reveals that the ξ obtained from all four codes is greater than one. This discrepancy arises from the model's omission of the shear span-to-depth ratio, longitudinal reinforcement ratio, and size effects, failing to accurately capture the shear mechanism in UHPC beams. Consequently, there is a pressing need for further research to refine the calculation methodologies.

Following an analytical examination of parameter influences and code calculation methodologies, this paper introduces an improved formula for the shear capacity computation of UHPC beams, drawing from the French code. This revised equation incorporates a fiber influence coefficient and a shear span-to-depth ratio correction factor for inclined sections, attentively considering the effects of the shear span ratio, steel fiber attributes, and fiber–matrix bond strength. The database's experimental-to-calculated value ratio has a mean of 1.3 with a standard deviation of 0.74, indicative of the modified equation's enhanced precision and broader applicability.

Based on the synthesis of existing research findings, it is evident that forthcoming investigations concerning the shear performance of UHPC beams will be directed towards several pivotal areas: the impact of fiber characteristics on the intrinsic material properties and shear resistance of UHPC; developing and analyzing sophisticated finite element models; evaluating the effects of long-term performance when subjected to environmental factors such as temperature fluctuations, humidity variations, and freeze–thaw cycles; and enhancing the precision and scope of design methodologies and standards. The limitations are cost and feasibility issues, the accuracy of finite element models, and the applicability of design methods.

Author Contributions: The conceptualization, methodology, and editorial review of this paper were carried out by Y.H., and data collection, writing, and analysis and validation were carried out by G.Y. All authors have read and agreed to the published version of the manuscript.

Funding: This research was funded by the National Natural Science Foundation of China (No. 51890901) and the Natural Science Foundation of Hunan Province, China (No. 2020RC50052020JJ2003).

Data Availability Statement: The data presented in this study are available on request from the corresponding author.

Conflicts of Interest: The authors declare no conflicts of interest.

References

1. de Larrard, F.; Sedran, T. Optimization of ultra-high-performance concrete by the use of a packing model. *Cem. Concr. Res.* **1994**, *24*, 997–1009. [CrossRef]
2. Shi, C.; Wu, Z.; Xiao, J.; Wang, D.; Huang, Z.; Fang, Z. A review on ultra high performance concrete: Part I. Raw materials and mixture design. *Constr. Build. Mater.* **2015**, *101*, 741–751. [CrossRef]
3. Wang, D.; Shi, C.; Wu, Z.; Xiao, J.; Huang, Z.; Fang, Z. A review on ultra high performance concrete: Part II. Hydration, microstructure and properties. *Constr. Build. Mater.* **2015**, *96*, 368–377. [CrossRef]

4. Wang, X.; Wu, D.; Geng, Q.; Hou, D.; Wang, M.; Li, L.; Wang, P.; Chen, D.; Sun, Z. Characterization of sustainable ultra-high performance concrete (UHPC) including expanded perlite. *Constr. Build. Mater.* **2021**, *303*, 124245. [CrossRef]
5. Yalçınkaya, Ç.; Çopuroğlu, O. Hydration heat, strength and microstructure characteristics of UHPC containing blast furnace slag. *J. Build. Eng.* **2021**, *34*, 101915. [CrossRef]
6. Gu, C.; Ye, G.; Sun, W. Ultrahigh performance concrete-properties, applications and perspectives. *Sci. China Technol. Sci.* **2015**, *58*, 587–599. [CrossRef]
7. Shao, Y.; Billington Sarah, L. Impact of UHPC Tensile Behavior on Steel Reinforced UHPC Flexural Behavior. *J. Struct. Eng.* **2022**, *148*, 04021244. [CrossRef]
8. Reddy, G.G.; Perumal, R. Influence of alccofine incorporation on the mechanical behavior of ultra-high performance concrete (UHPC). *Mater. Today Proc.* **2020**, *33*, 789–797. [CrossRef]
9. Li, S.; Jensen, O.M.; Yu, Q. Mechanism of rate dependent behaviour of ultra-high performance fibre reinforced concrete containing coarse aggregates under flexural loading. *Constr. Build. Mater.* **2021**, *301*, 124055. [CrossRef]
10. Gong, J.; Ma, Y.; Fu, J.; Hu, J.; Ouyang, X.; Zhang, Z.; Wang, H. Utilization of fibers in ultra-high performance concrete: A review. *Compos. Part B Eng.* **2022**, *241*, 109995. [CrossRef]
11. Pyo, S.; Kim, H.-K.; Lee, B.Y. Effects of coarser fine aggregate on tensile properties of ultra high performance concrete. *Cem. Concr. Compos.* **2017**, *84*, 28–35. [CrossRef]
12. Norhasri, M.S.M.; Hamidah, M.S.; Fadzil, A.M. Inclusion of nano metaclayed as additive in ultra high performance concrete (UHPC). *Constr. Build. Mater.* **2019**, *201*, 590–598. [CrossRef]
13. Muhd Norhasri, M.S.; Hamidah, M.S.; Mohd Fadzil, A.; Megawati, O. Inclusion of nano metakaolin as additive in ultra high performance concrete (UHPC). *Constr. Build. Mater.* **2016**, *127*, 167–175. [CrossRef]
14. Shafieifar, M.; Farzad, M.; Azizinamini, A. Experimental and numerical study on mechanical properties of Ultra High Performance Concrete (UHPC). *Constr. Build. Mater.* **2017**, *156*, 402–411. [CrossRef]
15. Kusumawardaningsih, Y.; Fehling, E.; Ismail, M. UHPC Compressive Strength Test Specimens: Cylinder or Cube? *Procedia Eng.* **2015**, *125*, 1076–1080. [CrossRef]
16. Tafraoui, A.; Escadeillas, G.; Vidal, T. Durability of the Ultra High Performances Concrete containing metakaolin. *Constr. Build. Mater.* **2016**, *112*, 980–987. [CrossRef]
17. Ahlborn, T.M.; Harris, D.K.; Misson, D.L.; Peuse, E.J. Characterization of Strength and Durability of Ultra-High-Performance Concrete under Variable Curing Conditions. *Transp. Res. Rec.* **2011**, *2251*, 68–75. [CrossRef]
18. Alkaysi, M.; El-Tawil, S.; Liu, Z.; Hansen, W. Effects of silica powder and cement type on durability of ultra high performance concrete (UHPC). *Cem. Concr. Compos.* **2016**, *66*, 47–56. [CrossRef]
19. Alhoubi, Y.; Mahaini, Z.; Abed, F. The Flexural Performance of BFRP-Reinforced UHPC Beams Compared to Steel and GFRP-Reinforced Beams. *Sustainability* **2022**, *14*, 15139. [CrossRef]
20. Chen, C.; Cai, H.Y.; Cheng, L.J. Shear Strengthening of Corroded RC Beams Using UHPC-FRP Composites. *J. Bridge Eng.* **2021**, *26*. [CrossRef]
21. Hong, S.G.; Lim, W.Y. Strengthening of shear-dominant reinforced concrete beams with ultra-high-performance concrete jacketing. *Constr. Build. Mater.* **2023**, *365*, 130043. [CrossRef]
22. Sneed, L.H.; Verre, S.; Ombres, L.; Carloni, C. Flexural behavior RC beams strengthened and repaired with SRP composite. *Eng. Struct.* **2022**, *258*, 114084. [CrossRef]
23. Zhang, P.; Xu, F.; Liu, Y.; Sheikh, S.A. Shear behaviour of composite beams with permanent UHPC formwork and high-strength steel rebar. *Constr. Build. Mater.* **2022**, *352*, 128951. [CrossRef]
24. Hosseinzadehfard, E.; Mobaraki, B. Investigating concrete durability: The impact of natural pozzolan as a partial substitute for microsilica in concrete mixtures. *Constr. Build. Mater.* **2024**, *419*, 135491. [CrossRef]
25. Mobaraki, B.; Ma, H.; Lozano Galant, J.A.; Turmo, J. Structural Health Monitoring of 2D Plane Structures. *Appl. Sci.* **2021**, *11*, 2000. [CrossRef]
26. Hou, R.; Hou, Q. Prediction of the shear capacity of ultrahigh-performance concrete beams using neural network and genetic algorithm. *Sci. Rep.* **2023**, *13*, 2145. [CrossRef] [PubMed]
27. Ma, K.; Ma, Y.; Xing, G.; Liu, B. Study on shear performance of reinforced ultra-high performance concrete beams. *J. Build. Struct.* **2022**, *43*, 179–188. (In Chinese) [CrossRef]
28. Zhou, M.; Lu, W.; Song, J.; Lee, G.C. Application of Ultra-High Performance Concrete in bridge engineering. *Constr. Build. Mater.* **2018**, *186*, 1256–1267. [CrossRef]
29. Wu, P.; Wu, C.; Liu, Z.; Hao, H. Investigation of shear performance of UHPC by direct shear tests. *Eng. Struct.* **2019**, *183*, 780–790. [CrossRef]
30. Ma, X.; Chen, B.; Yang, Y.; Huang, Q.; Su, J.; Wu, Q.; Shen, X. Calculation method of shear capacity of R-UHPC beams. *J. Transp. Eng.* **2017**, *17*, 16–26. (In Chinese)
31. Pourbaba, M.; Joghataie, A. Determining shear capacity of ultra-high performance concrete beams by experiments and comparison with codes. *Sci. Iran.* **2019**, *26*, 273–282. [CrossRef]
32. Pourbaba, M.; Joghataie, A.; Mirmiran, A. Shear behavior of ultra-high performance concrete. *Constr. Build. Mater.* **2018**, *183*, 554–564. [CrossRef]

33. Yang, J.; Doh, J.-H.; Yan, K.; Zhang, X. Experimental investigation and prediction of shear capacity for UHPC beams. *Case Stud. Constr. Mater.* **2022**, *16*, e01097. [CrossRef]
34. Luo, D.; Lu, T.; Chen, Y.F. Application of ultra-high-performance concrete in prefabricated buildings. *Mater. Test.* **2021**, *63*, 1174–1183. [CrossRef]
35. Zhang, H.-X.; Zhou, M.; Feng, W.; Wen, J. Application of Ultra-high Performance Concrete in Lifeline Engineering. *DEStech Trans. Eng. Technol. Res.* **2017**. [CrossRef]
36. Akhnoukh, A.K.; Buckhalter, C. Ultra-high-performance concrete: Constituents, mechanical properties, applications and current challenges. *Case Stud. Constr. Mater.* **2021**, *15*, e00559. [CrossRef]
37. Bajaber, M.A.; Hakeem, I.Y. UHPC evolution, development, and utilization in construction: A review. *J. Mater. Res. Technol.* **2021**, *10*, 1058–1074. [CrossRef]
38. Xue, J.; Briseghella, B.; Huang, F.; Nuti, C.; Tabatabai, H.; Chen, B. Review of ultra-high performance concrete and its application in bridge engineering. *Constr. Build. Mater.* **2020**, *260*, 119844. [CrossRef]
39. Xia, J.; Mackie, K.R.; Saleem, M.A.; Mirmiran, A. Shear failure analysis on ultra-high performance concrete beams reinforced with high strength steel. *Eng. Struct.* **2011**, *33*, 3597–3609. [CrossRef]
40. Zagon, R.; Zoltan, K. Shear Behaviour of UHPC Concrete Beams. *Procedia Technol.* **2016**, *22*, 122–126. [CrossRef]
41. Lantsoght, E.O.L. How do steel fibers improve the shear capacity of reinforced concrete beams without stirrups? *Compos. Part B Eng.* **2019**, *175*, 107079. [CrossRef]
42. Xu, Q.; Zhu, Y.; Wang, J.; Sebastian, W. Effectiveness and response of replacing web reinforcements with steel fibers reinforced in shear for non-stirrup UHPC beams. *Eng. Struct.* **2023**, *288*, 116168. [CrossRef]
43. Yoo, D.-Y.; Yuan, T.; Yang, J.-M.; Yoon, Y.-S. Feasibility of replacing minimum shear reinforcement with steel fibers for sustainable high-strength concrete beams. *Eng. Struct.* **2017**, *147*, 207–222. [CrossRef]
44. Jin, L.; Zhou, J.; Li, Y.; Cao, X.; Fu, Q. Experimental study on shear performance of beams with high-strength reinforced reactive powder concrete. *J. Build. Struct.* **2015**, *36*, 277–285. (In Chinese) [CrossRef]
45. Chen, B.; Wu, Q.; Huang, Q.; Ma, X.; Su, J. Experimental study on shear performance of reinforced ultra-high performance concrete beams. *J. Fuzhou Univ. Nat. Sci. Ed.* **2018**, *46*, 512–517. (In Chinese)
46. Luo, M. Experimental and Theoretical Study on Mechanical Properties and Bearing Capacity of Ultra High Performance Concrete Members. Ph.D. Thesis, Lanzhou Jiaotong University, Lanzhou, China, 2021. (In Chinese)
47. Chen, B.; Zhou, J.; Zhang, D.; Su, J.; Nuti, C.; Sennah, K. Experimental study on shear performances of ultra-high performance concrete deep beams. *Structures* **2022**, *39*, 310–322. [CrossRef]
48. Zhou, L.; Wan, S. Shear behavior of UHPC beams with small shear span to depth ratios based on MSTM. *Case Stud. Constr. Mater.* **2022**, *16*, e01134. [CrossRef]
49. Lim, W.-Y.; Hong, S.-G. Shear Tests for Ultra-High Performance Fiber Reinforced Concrete (UHPFRC) Beams with Shear Reinforcement. *Int. J. Concr. Struct. Mater.* **2016**, *10*, 177–188. [CrossRef]
50. Gao, C.; Tang, T. Study on the influence of size effect on the shear performance of UHPC beams without web reinforcement. *Build. Struct.* **2022**, *52*, 1435–1441. (In Chinese) [CrossRef]
51. Ngo, T.T.; Park, J.K.; Pyo, S.; Kim, D.J. Shear resistance of ultra-high-performance fiber-reinforced concrete. *Constr. Build. Mater.* **2017**, *151*, 246–257. [CrossRef]
52. Son, J.; Beak, B.; Choi, C. Experimental study on shear strength for ultra-high performance concrete beam. In Proceedings of the 18th International Conference on Composites Materials, Jeju, Republic of Korea, 21 August 2011.
53. Aziz, O.; Hasan, M.; Ali, H. Shear Strength and Behavior of Ultra-High Performance Fiber Reinforced Concrete (UHPC) Deep Beams without Web Reinforcement. *Int. J. Civ. Eng.* **2013**, *2*, 85–96.
54. Fahmi, H.; Alshaarbaf, I.; Ahmed, A. Behavior of Reactive Powder Concrete Deep Beams. *AL-Mansour J.* **2013**, *20*, 1–22.
55. Chen, B.; Zhou, J.; Zhang, D.; Sennah, K.; Nuti, C. Shear performances of reinforced ultra-high performance concrete short beams. *Eng. Struct.* **2023**, *277*, 115407. [CrossRef]
56. Wang, Q.; Song, H.-L.; Lu, C.-L.; Jin, L.-Z. Shear performance of reinforced ultra-high performance concrete rectangular section beams. *Structures* **2020**, *27*, 1184–1194. [CrossRef]
57. Bermudez, M.; Hung, C.C. Shear behavior of ultra-high performance hybrid fiber reinforced concrete beams. In Proceedings of the International Interactive Symposium on Ultra-High Performance Concrete, Albany, NY, USA, 2–5 June 2019.
58. Yavaş, A.; Hasgul, U.; Turker, K.; Birol, T. Effective fiber type investigation on the shear behavior of ultrahigh-performance fiber-reinforced concrete beams. *Adv. Struct. Eng.* **2019**, *22*, 1591–1605. [CrossRef]
59. Yaseen, S. An Experimental Study on the Shear Strength of High-performance Reinforced Concrete Deep Beams without Stirrups. *Eng. Technol. J.* **2016**, *34*, 2123–2139. [CrossRef]
60. Ridha, M.M.S.; Sarsam, K.F.; Al-Shaarbaf, I.A.S. Experimental Study and Shear Strength Prediction for Reactive Powder Concrete Beams. *Case Stud. Constr. Mater.* **2018**, *8*, 434–446. [CrossRef]
61. Li, P.; Cheng, Q.; Chen, N.; Tian, Y.; Fang, J.; Jiang, H. Experimental Study on Shear Behavior of Non-Stirrup Ultra-High Performance Concrete Beams. *Materials* **2023**, *16*, 4177. [CrossRef]
62. Diao, B.; Feng, Y.; Ye, Y.; Yang, S. Study on shear performance of reinforced ultra-high performance hybrid steel fibre concrete beams. *Ind. Build.* **2012**, *42*, 6–10+15. (In Chinese) [CrossRef]

63. Zhang, Y. Study on the Load Carrying Capacity of Inclined Section of Ultra-High Performance Concrete Beams at Room Temperature. Master's Thesis, Shandong University of Architecture, Jinan, China, 2020. (In Chinese)
64. Zhong, H. Study on Shear Performance of UHPC Beams without Web Reinforcement. Master's Thesis, South China University of Technology, Guangzhou, China, 2021. (In Chinese)
65. Qi, J.; Wang, J.; Feng, Y. Shear performance of an innovative UHPFRC deck of composite bridge with coarse aggregate. *Adv. Concr. Constr.* **2019**, *7*, 219–229. [CrossRef]
66. Luo, B.G.; Qin, H.E.; Jin, L.C. Study on shear bearing capacity of activated powder concrete beams based on truss arch model. *Build. Sci.* **2016**, *32*, 1–7. (In Chinese) [CrossRef]
67. Cao, X.; Wang, H.; Zhang, Y.; Zhang, J. Neural network-based prediction of shear capacity of activated powder concrete beams. *J. Henan Univ. Sci. Technol. Nat. Sci. Ed.* **2017**, *38*, 63–68+67. (In Chinese) [CrossRef]
68. Jin, L.; Liang, X.; Zhang, Y.; Zhang, M. Research on shear performance of high-strength reinforced ultra-high performance concrete beams with different shear-to-span ratios. *Ind. Build.* **2018**, *48*, 57–62. (In Chinese) [CrossRef]
69. Wang, Z.; Shao, Z.; Liang, X.; Cao, Z.; Wu, K.; Zhao, N. Detailed multi-mechanism shear modelling of reinforced ultra-high performance concrete beams. *J. Build. Struct.* **2024**, *45*, 217–229. (In Chinese) [CrossRef]
70. Mohammed, M. Shear Behavior of Reactive Powder Concrete Beams with and without Coarse Aggregate. *AUT J. Civ. Eng.* **2018**, *2*, 87–96. [CrossRef]
71. Kamal, M.M.; Safan, M.A.; Etman, Z.A.; Salama, R.A. Behavior and strength of beams cast with ultra high strength concrete containing different types of fibers. *HBRC J.* **2014**, *10*, 55–63. [CrossRef]
72. Al-Alawi, A.R.; Mashrei, M.A. Shear capacity of sustainable ultra-high performance concrete beam reinforced with macro synthetic fiber as a sustainable alternative for stirrups and steel fiber. *Case Stud. Constr. Mater.* **2022**, *17*, e01443. [CrossRef]
73. Hasgül, U.; Yavas, A.; Birol, T. Replacement of Stirrups by Steel Fibers in Shear Dominant UHPFRC Beams. *Turk. J. Civ. Eng.* **2023**, *34*, 103–124. [CrossRef]
74. Abbas, Y.; Shafiq, N.; Fares, G.; Osman, M.; Khan, M.I.; Khatib, J. Strength Iso-Responses of Shear-Deficient Ultra-High Performance Fiber Reinforced Concrete Beams. *Sustainability* **2023**, *15*, 4265. [CrossRef]
75. Yang, J.; Yan, K.; Doh, J.-H.; Zhang, X. Experimental study on shear performance of ultra-high-performance concrete beams at elevated temperatures. *Eng. Struct.* **2023**, *291*, 116304. [CrossRef]
76. Qi, J.N.; Wang, J.Q.; Zhou, K.; Liu, J.Z.; Li, W.C. Shear performance test and shear bearing capacity calculation method for UHPC beams. *Chin. J. Highw.* **2020**, *33*, 95–103. (In Chinese) [CrossRef]
77. Jabbar, A.M.; Hamood, M.J.; Mohammed, D.H. The effect of using basalt fibers compared to steel fibers on the shear behavior of ultra-high performance concrete T-beam. *Case Stud. Constr. Mater.* **2021**, *15*, e00702. [CrossRef]
78. Shu, Y. Experimental study on inclined section shear performance of coarse aggregate UHPC beams. *Sichuan Constr.* **2020**, *40*, 302–305. (In Chinese)
79. Qi, J.; Ma, Z.J.; Wang, J. Shear Strength of UHPFRC Beams: Mesoscale Fiber-Matrix Discrete Model. *J. Struct. Eng.* **2017**, *143*, 04016209. [CrossRef]
80. Ou, C.-X. Shear Performance Test and Shear Capacity Modelling of UHPC Beams. Master's Thesis, Southeast University, Nanjing, China, 2022. (In Chinese)
81. Ji, W.; Li, W.; An, M.; Zhu, L. Shear Capacity of T-Section Girders Made of Reactive Powder Concrete. *J. Bridge Eng.* **2018**, *23*, 04018041. [CrossRef]
82. Qi, J.; Ding, X.; Wang, Z.; Hu, Y. Shear strength of fiber-reinforced high-strength steel ultra-high-performance concrete beams based on refined calculation of compression zone depth considering concrete tension. *Adv. Struct. Eng.* **2019**, *22*, 2006–2018. [CrossRef]
83. Li, H.-D. Experimental Study on the Diagonal Cross-Section Shear Performance of Coarse Aggregate UHPC Beams. Master's Thesis, Southwest Jiaotong University, Chengdu, China, 2018. (In Chinese)
84. Chen, B. Study on Shear Performance Of Prestressed RPC Beams. Master's Thesis, Hunan University, Changsha, China, 2007. (In Chinese)
85. Cao, X.; Quan, Y.; Yang, Z.; Jin, Q.; Zheng, Y. Experimental study of size effect on shear performance of ultra-high performance concrete beams. *J. Taiyuan Univ. Technol.* **2023**, *54*, 500–508. (In Chinese) [CrossRef]
86. Wu, X.; Han, S.-M. First Diagonal Cracking and Ultimate Shear of I-Shaped Reinforced Girders of Ultra High Performance Fiber Reinforced Concrete without Stirrup. *Int. J. Concr. Struct. Mater.* **2009**, *3*, 47–56. [CrossRef]
87. Mészöly, T.; Randl, N. Shear behavior of fiber-reinforced ultra-high performance concrete beams. *Eng. Struct.* **2018**, *168*, 119–127. [CrossRef]
88. Yavas, A.; Goker, C.O. Impact of Reinforcement Ratio on Shear Behavior of I-Shaped UHPC Beams with and without Fiber Shear Reinforcement. *Materials* **2020**, *13*, 1525. [CrossRef]
89. Ţibea, C.; Bompa, D.V. Ultimate shear response of ultra-high-performance steel fibre-reinforced concrete elements. *Arch. Civ. Mech. Eng.* **2020**, *20*, 49. [CrossRef]
90. Cao, X.; Ren, Y.; Lian, D.; Jin, L.; Li, L.; He, D. Shear performance test of different types of steel fibre UHPC beams without web. *J. Guilin Univ. Technol.* **2024**, *44*, 67–74. (In Chinese)
91. Baby, F.; Marchand, P.; Toutlemonde, F. Shear Behavior of Ultrahigh Performance Fiber-Reinforced Concrete Beams. I: Experimental Investigation. *J. Struct. Eng.* **2014**, *140*, 04013111. [CrossRef]

92. Pansuk, W.; Nguyen, T.N.; Sato, Y.; Den Uijl, J.A.; Walraven, J.C. Shear capacity of high performance fiber reinforced concrete I-beams. *Constr. Build. Mater.* **2017**, *157*, 182–193. [CrossRef]
93. Feng, J.; Li, P.; Wu, J.; Jiang, H.; Tian, Y.; Sun, X. Shear behavior of externally prestressed UHPC beams without stirrups. *Case Stud. Constr. Mater.* **2023**, *18*, e01766. [CrossRef]
94. Ye, M.; Li, L.; Pei, B.; Yoo, D.-Y.; Li, H. Shear behavior of externally prestressed ultra-high-performance concrete (UHPC) T-beams without stirrups. *Eng. Struct.* **2023**, *288*, 116217. [CrossRef]
95. Hegger, J.; Bertram, G. Shear carrying capacity of ultra-high performance concrete beams. In *Tailor Made Concrete Structures*; CRC Press: London, UK, 2008.
96. Jiang, H.; Feng, J.; Xiao, J.; Tian, Y.; Sun, X.; Chen, Z. Experimental exploration of shear performance of extracorporeally prestressed webless ultra-high performance concrete beams. *J. Compos. Mater.* **2022**, *39*, 707–717. (In Chinese) [CrossRef]
97. Jia, L.; Fang, Z.; Guadagnini, M.; Pilakoutas, K.; Huang, Z. Shear behavior of ultra-high-performance concrete beams prestressed with external carbon fiber-reinforced polymer tendons. *Front. Struct. Civ. Eng.* **2021**, *15*, 1426–1440. [CrossRef]
98. Voo Yen, L.; Poon Wai, K.; Foster Stephen, J. Shear Strength of Steel Fiber-Reinforced Ultrahigh-Performance Concrete Beams without Stirrups. *J. Struct. Eng.* **2010**, *136*, 1393–1400. [CrossRef]
99. Voo, Y.; Foster, S.; Gilbert, R. Shear Strength of Fiber Reinforced Reactive Powder Concrete Prestressed Girders without Stirrups. *J. Adv. Concr. Technol.* **2006**, *4*, 123–132. [CrossRef]
100. Jin, L.; Wang, L.; Zhou, J.; Wang, H.; Li, Y. Experimental study on shear performance of partially prestressed UHPC thin web girders without web reinforcement. *J. Railw.* **2019**, *41*, 105–116. (In Chinese)
101. Yang, I.-H.; Joh, C.; Kim, B.-S. Shear behaviour of ultra-high-performance fibre-reinforced concrete beams without stirrups. *Mag. Concr. Res.* **2012**, *64*, 979–993. [CrossRef]
102. Ji, W.Y.; Ding, B.; An, M.C. Experimental study on shear resistance of activated powder concrete T-beam. *China Railw. Sci.* **2011**, *32*, 38–42. (In Chinese)
103. Thiemicke, J.; Fehling, E. *Experimental and Numerical Investigations on I-Shaped UHPC-Beams with Combined Reinforcement under Shear Load*; CRC Press: London, UK, 2016; pp. 1363–1367.
104. Kodur, V.; Solhmirzaei, R.; Agrawal, A.; Aziz, E.M.; Soroushian, P. Analysis of flexural and shear resistance of ultra high performance fiber reinforced concrete beams without stirrups. *Eng. Struct.* **2018**, *174*, 873–884. [CrossRef]
105. Shahnewaz, M.; Rteil, A.; Alam, M.S. Shear strength of reinforced concrete deep beams—A review with improved model by genetic algorithm and reliability analysis. *Structures* **2020**, *23*, 494–508. [CrossRef]
106. Tong, L.; Xiao, S.; He, L.; Zhang, Y.; Zhao, X.-L. Fatigue behavior of steel reinforced concrete (SRC) beams with different shear span-to-depth ratios. *Eng. Struct.* **2018**, *166*, 339–353. [CrossRef]
107. Arowojolu, O.; Ibrahim, A.; Almakrab, A.; Saras, N.; Nielsen, R. Influence of Shear Span-to-Effective Depth Ratio on Behavior of High-Strength Reinforced Concrete Beams. *Int. J. Concr. Struct. Mater.* **2021**, *15*, 14. [CrossRef]
108. Zhang, C.; Zhang, B.S.; Huang, J.F. Investigation on shear strength of reinforced concrete beams without web reinforcement. *J. Civ. Environ. Eng.* **2005**, *27*, 48–52.
109. Smarzewski, P.; Barnat-Hunek, D. Effect of Fiber Hybridization on Durability Related Properties of Ultra-High Performance Concrete. *Int. J. Concr. Struct. Mater.* **2017**, *11*, 315–325. [CrossRef]
110. Wu, Z.; Shi, C.; Khayat, K.H. Investigation of mechanical properties and shrinkage of ultra-high performance concrete: Influence of steel fiber content and shape. *Compos. Part B Eng.* **2019**, *174*, 107021. [CrossRef]
111. Wang, L.; Zhang, X.; Zhang, J.; Ma, Y.; Liu, Y. Effects of stirrup and inclined bar corrosion on shear behavior of RC beams. *Constr. Build. Mater.* **2015**, *98*, 537–546. [CrossRef]
112. Ahmad, S.; Bahij, S.; Al-Osta, M.A.; Adekunle, S.K.; Al-Dulaijan, S.U. Shear Behavior of Ultra-High-Performance Concrete Beams Reinforced with High-Strength Steel Bars. *ACI Struct. J.* **2019**, *116*, 3–14. [CrossRef]
113. El-Helou Rafic, G.; Graybeal Benjamin, A. Shear Behavior of Ultrahigh-Performance Concrete Pretensioned Bridge Girders. *J. Struct. Eng.* **2022**, *148*, 04022017. [CrossRef]
114. Yoo, D.-Y.; Banthia, N.; Kang, S.-T.; Yoon, Y.-S. Size effect in ultra-high-performance concrete beams. *Eng. Fract. Mech.* **2016**, *157*, 86–106. [CrossRef]
115. Hussein, L.; Amleh, L. Size effect of ultra-high performance fiber reinforced concrete composite beams in shear. *Struct. Concr.* **2018**, *19*, 141–151. [CrossRef]
116. Yoo, D.-Y.; Yang, J.-M. Effects of stirrup, steel fiber, and beam size on shear behavior of high-strength concrete beams. *Cem. Concr. Compos.* **2018**, *87*, 137–148. [CrossRef]
117. *NF P 18-710*; National Addition to Eurocode 2—Design of Concrete Structures: Specific Rules for Ultra-High Performance Fibre-Reinforced Concrete (UHPFRC). AFNOR, France Standard Institute: Paris, France, 2016.
118. Japan Society of Civil Engineers. *Recommendations for Design and Construction of High Performance Fiber Reinforced Cement Composites with Multiple Fine Cracks (HPFRCC)*; Japan Society of Civil Engineers: Tokyo, Japan, 2008.
119. EPFL-Swiss Federal Institute of Technology MCS-Maintenance. *Ultra-High Performance Fibre Reinforced Cement-Based Composites (UHPFRC) Construction Material*; EPFL: Lausanne, Switzerland, 2016.
120. KICT. *Design Guidelines for K-UHPC*; Korea Concrete Institute: Seoul, Republic of Korea, 2014.
121. Crane, C.K. Shear and Shear Friction of Ultra-High Performance Concrete Bridge Girders. Ph.D. Thesis, Georgia Institute of Technology, Atlanta, GA, USA, 2010.

122. Li, L. Research on Shear Performance and Calculation Method of UHPC Composite Beams without Web Reinforcement. Master's Thesis, Southeast University, Nanjing, China, 2021. (In Chinese)
123. Tahenni, T.; Chemrouk, M.; Lecompte, T. Effect of steel fibers on the shear behavior of high strength concrete beams. *Constr. Build. Mater.* **2016**, *105*, 14–28. [CrossRef]
124. Qi, J.; Cheng, Z.; John Ma, Z.; Wang, J.; Liu, J. Bond strength of reinforcing bars in ultra-high performance concrete: Experimental study and fiber–matrix discrete model. *Eng. Struct.* **2021**, *248*, 113290. [CrossRef]
125. Singh, H. Flexural Modeling of Steel Fiber-Reinforced Concrete Members: Analytical Investigations. *Pract. Period. Struct. Des. Constr.* **2014**, 20–30. [CrossRef]
126. *DBJ 43/T 325-2017*; Technical Specification for Reactive Powder Concrete Structures. China Architecture & Building Press: Beijing, China, 2018. (In Chinese)